Dalton Transactions

Facile Hydrogen Atom Abstraction and Sulfide Formation in a Methyl-Thiolate Capped Iron-Sulfur-Carbonyl Cluster

Journal:	*Dalton Transactions*
Manuscript ID	DT-COM-10-2019-004098.R1
Article Type:	Communication
Date Submitted by the Author:	25-Nov-2019
Complete List of Authors:	Shupp, John; The University of Texas at Austin, Chemistry Rose, Michael; The University of Texas at Austin,

COMMUNICATION

Facile Hydrogen Atom Abstraction and Sulfide Formation in a Methyl-Thiolate Capped Iron-Sulfur-Carbonyl Cluster

Received 00th January 20xx,
Accepted 00th January 20xx

DOI: 10.1039/x0xx00000x

J. Patrick Shupp and Michael J. Rose*

ORCIDs
Shupp: 0000-0001-5176-5677
Rose: 0000-0002-6960-6639

The interest in methyl group C–H bond activation near or bound to iron-containing clusters is of key biological importance, due to the broad relavence of radical SAM reactions. Specifically, such processes are implicated in the biogenesis of the interstitial carbide found in the nitrogenase FeMoco active site. In this work, we find that the diamagnetic, methyl-thiolate capped iron-carbonyl cluster anion $[(CH_3S)Fe_3(CO)_9]^-$ (1) undergoes facile C–H hydrogen atom abstraction upon treatment with TEMPO. The process leads to (*i*) eradication of the CH_3 moeity, (*ii*) formation of a sulfide bridge, and (*iii*) cluster dimerization — thereby generating the 'dimer of trimers' cluster $[K(benzo\text{-}15\text{-}crown\text{-}5)_2]_2[(SFe_2(CO)_{12})_2Fe(CO)_2]$ (2). In contrast, the corresponding isopropyl variant $[Fe_3(S^iPr)(CO)_9]^-$ (3) *does not react with TEMPO*. Mass spectrometry confirmed the presence of TEMPOH, as well as CO oxidation vis a vis CO_2 and 2,2,6,6-tetramethylpiperidine. GC-MS measurements of the headspace reveal that the ultimate fate of the methyl carbon is likely incorporation into multiple products — one of which may be a volatile low mass hydrocarbon — rather than carbon/carbide incorporation.

The biogenesis of the M cluster in nitrogenase has garnered much interest since the identification of the interstitial carbide in 2011.[1,2] The unique motif of a 6-coordinate C^{4-} bound to the six iron centers present in FeMoco/FeVco are the only known examples in biological systems,[3] and few examples exist in chemical systems.[4–7] The Nif class of enzymes has been shown to perform the wide variety of transformations necessary to generate the nitrogenase cofactor. NifS and NifU, the first enzymes in the series, convert cysteinal thiolates to inorganic $[Fe_2S_2]$ and $[Fe_4S_4]$ clusters.[8] Ribbe and coworkers have elucidated much of the mechanism of carbide insertion through a clever fusion protein of NifEN-B, a construct which combines the scaffold protein NifEN with the radical S-adenosyl methionine (SAM) enzyme NifB.[9]

In other work, it was shown that carbide formation requires two equivalents of SAM; one for methyl group donation (which eventually becomes the carbide), and a second for radical abstraction of a hydrogen atom.[10] The initial binding site of the methyl group was also traced by HPLC and GCMS, revealing that the methyl group first binds to a sulfide in the native enzyme.[11] Furthermore, it was observed that R group transfer occurs before any radical reactions, likely through a simple S_N2-type reaction. The subsequent radical abstraction of a hydrogen atom then allows for a radical-electron induced rearrangement of the iron clusters.[12] This Provides a stimulus for investigating the reactivity of methyl substituted iron-sulfur clusters with a radical initiator. Relatedly, oxidation of NifEN-B with indigo disulfonate resulted in cessation of all methyl transfer activity, suggesting that the sulfide must be sufficiently anionic and/or poised at a sufficiently negative potential for the reaction to proceed.

We recently reported reduced clusters of general formula $K[S_lFe_m(CO)_n]$ (l = 1-4, m = 2-4, n = 7-12) that could serve as non-enzymatic models for both the methyl substitution (S_N2) and subsequent radical reaction. These clusters have the advantages of being significantly reduced, as well as having an alkali cation that is not susceptible to radical chemistry.[13] Specifically, the cluster $K_2[SFe_3(CO)_9]$ (**1a**) was chosen, due to its versatility in substituting R groups using common electrophiles that can be installed on the S^{2-} 'bridgehead'. This approach makes it a suitable — albeit not entirely biomimetic — model system for investigating -SCH_3 reaction mechanisms associated with iron-containing clusters.

The University of Texas at Austin; Austin, TX 78758

*corresponding author: mrose@cm.utexas.edu
Electronic Supplementary Information (ESI) available: [details of any supplementary information available should be included here]. See DOI: 10.1039/x0xx00000x

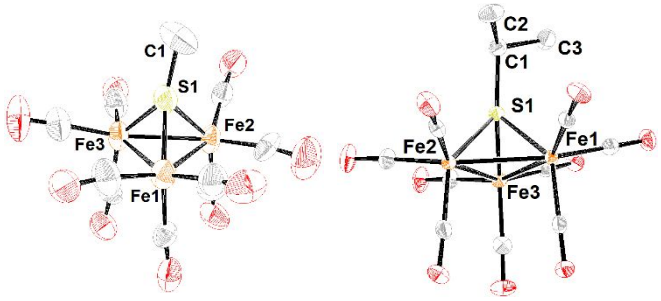

Fig. 1 ORTEP diagrams of $[K(benzo\text{-}15\text{-}crown\text{-}5)_2][S(CH_3)Fe_3(CO)_9]$ (**1**, 30% thermal ellipsoids) and $[K(benzo\text{-}15\text{-}crown\text{-}5)_2][S(C_3H_7Fe_3(CO)_9]$ (**3**, 50% thermal ellipsoids) at 100 K; counterions are omitted for clarity.

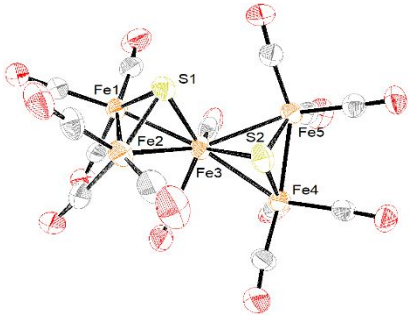

Fig. 2 ORTEP diagram (50% thermal ellipsoids) of $[K(benzo\text{-}15\text{-}crown\text{-}5)_2]_2[(SFe_2(CO)_{12})_2Fe(CO)_2]$ (**2**) at 100 K; counterions are omitted for clarity.

The methylation of $K_2[SFe_3(CO)_9]$ with CH_3I proceeded in a straightforward manner in THF at 0 °C to afford the mono-anionic product $K[(CH_3S)Fe_3(CO)_9]$ (**1**). After treatment with excess benzo-15-crown-5, dark red X-ray quality crystals were obtained (**Figure 1**). The resulting bond metrics were similar to those previously observed in $NEt_4[(CH_3S)Fe_3(CO)_9]$.[14] Importantly, the lack of easily dissociable protons or reactive C–H moieties in the K-crown counterion (unlike NEt_3H^+ or NEt_4^+) provided an ideal cluster for methyl C–H activation studies.

Since the starting material $K[(CH_3S)Fe_3(CO)_9]$ (**1**) contains multiple Fe centers capable of forming bridging hydrides, it was important to select a relatively mild H-atom abstraction reagent. Thus 2,2,6,6-tetramethyl-1-piperidinyloxy (TEMPO) was selected due to its mild O–H bond formation strength.[15] Reactions of the methylated cluster **1** with TEMPO in THF generated a red-brown color over the course of 2 hours. Following extraction of species in Et_2O (identified as the anionic fragment $[HFe_3CO_9]^-$, m/z = 420), the insoluble material was dissolved in MeCN, with excess benzo-15-crown-5 for crystallization. The product was identified as $[K(benzo\text{-}15\text{-}crown\text{-}5)_2]_2[(SFe_2(CO)_{12})_2Fe(CO)_2]$ (**2**) by single crystal X-ray diffraction (**Figure 2**). Cluster **2** reveals two key transformations: (*i*) S–CH_3 bond breakage to generate the inorganic sulfide, and (*ii*) the combination of two Fe_3 units (and extrusion of one Fe center) to form an S_2Fe_5 framework. Additionally, two electron oxidation of the Fe centers was observed (one electron from each progenitor cluster of **1**). The same product was obtained regardless of solvent identity (THF, MeCN, FPh) or temperature (–78 °C or ambient temperature). The bond metrics of the dianion **2** were similar to that observed previously in the PPh_4^+ and NEt_4^+ formulation of **2.**[16,17] which were synthesized by an entirely different route.

This process is bears some resemblance to the biosynthesis of the FeMoco active site, wherein the addition of SAM causes oxidation of the SAM-motif bound $[Fe_4S_4]^{1+}$ in NifB to an oxidized EPR silent intermediate;[9] in this process, S^{2-} and C^{4-} are ultimately generated as charged ligands, implying oxidation of the iron centers en route to the intermediate L cluster. Unfortunately, the incorporation of any carbon (or carbide) motif to the cluster was not observed in this work, although it was demonstrated that a radical electron can aid in the fusion of two iron-sulfur units.

It has been speculated that after the first hydrogen atom abstraction, the subsequent transformations to a carbide proceed by acid-base chemistry.[8] To test this hypothesis in our system, the same reaction was performed using two equivalents of a non-coordinating base (lutidine) at –78 °C (to prevent any deprotonation event prior to TEMPO addition. However, no changes in reaction outcome were observed.

Attempts using NMR to characterize the fate of the carbon atom using isotopically labeled $^{13}CH_3I$ and CD_3I proved unviable, as the reaction mixture exhibited paramagnetism. We deemed it likely that any products generated from a C_1 source not incorporated into a cluster could be gaseous at room temperature. Thus, headspace GC measurements of the reaction mixture were pursued (**Figure S1**), revealing two major peaks. CO_2 was identified as the first species (R_f = 9 min) by comparison to an internal standard, and is attributed to oxidation of CO by a TEMPO derivative, namely TEMPOH (m/z = 157, **Figure S3**). TEMPOH was presumed to participate in proton donation and hydride formation as suggested by detection of the cluster fragment $[HFe_3CO_9]^-$ in the reaction mixture (m/z = 420, **Figure S4**). The generated $TEMPO^-$ (m/z = 156, **Figure S3**) then induced CO oxidation to form CO_2, which is further supported by the detection of 2,2,6,6 tetramethylpiperidine (m/z = 140, 142, **Figure S3**).

The second gaseous species (R_f = 27 min) proved more perplexing. The peak height of this gas was roughly five times greater than that of CO_2. Solvent effects, particularly the incorporation of cyanide from MeCN, were excluded by performing the same experiment in fluorobenzene (**Figure S2**), which afforded the same pattern of gases and elution times.

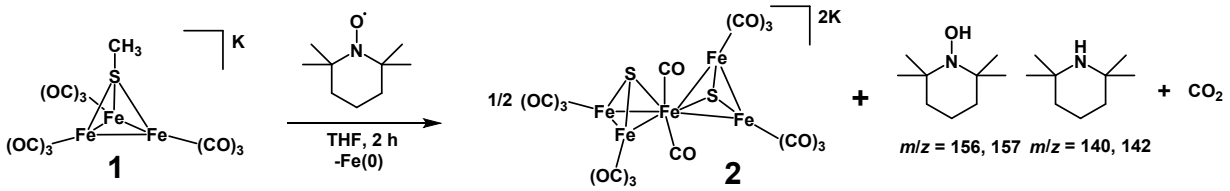

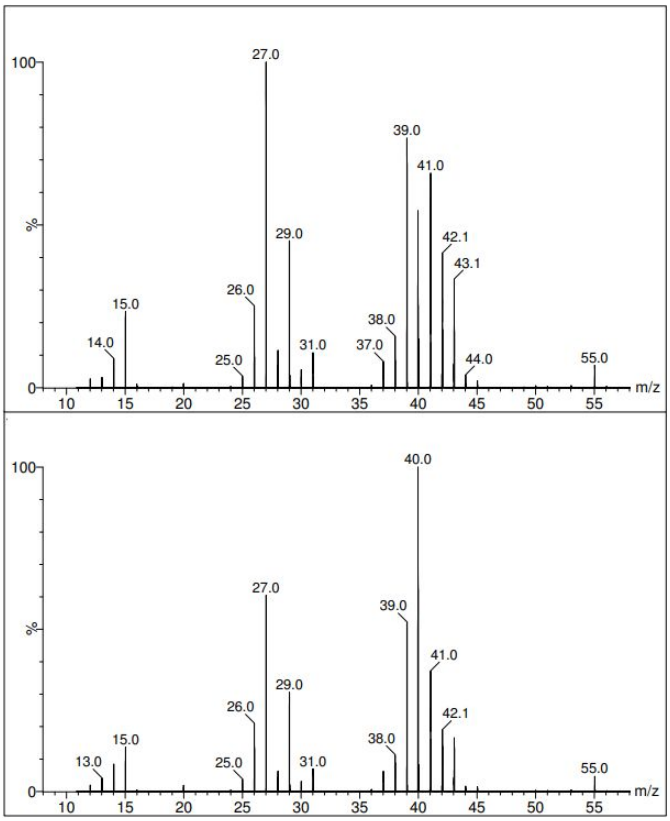

Fig. 3 Mass chromatograms of the headspace of the reaction between TEMPO and $K[(CD_3S)Fe_3(CO)_9]$ (*top*) and $K[(CH_3S)Fe_3(CO)_9]$ (*bottom*). Notably the peaks centered near *m/z* = 40 show significant changes.

Headspace MS performed in CI mode (**Figure 3**) revealed the *m/z* values for the two unknowns as 40 and 55. To further investigate these peaks, the deuterium labeled complex $K[(CD_3S)Fe_3(CO)_9]$ was prepared. While the peak at *m/z* = 55 remained unchanged, the peaks centered near *m/z* = 40 showed a different distribution of peak ratios. This indicates that deuterium was incorporated into the species corresponding to *m/z* = 40, and that this species originated from the isotopically labeled methyl group. Several reports have investigated the products and kinetics of methyl radicals with alkenes to form small carbon units.[18–22] An unambiguous result would have been a quantitative shift of all features near *m/z* = 40 to *m/z* = 42 or 44. However, since the shift in features occurred in a non-uniform manner, a direct assignment is not possible. It is likely that there is no single isotopic product that is generated from the methyl group, possibly due to H/D scrambling via solvent/radical processes. In fact, examination of the mass spectra of the reaction mixture (**Figures S3**, **S4**) reveals multiple products.

Lastly, we sought to determine the selectivity of the TEMPO-driven reaction for the methyl group, in particular. Thus we investigated H-atom abstraction using a cluster with just a single α-proton, namely the isopropyl analog $K[(^iPrS)Fe_3(CO)_9]$ (**3**), whose X-ray structure is depicted in **Figure 1**. Intriguingly, reaction of **3** with TEMPO in any solvent, (THF, MeCN, FPh) and at any temperature (–78 °C to ambient) provided no evidence of any reaction. In fact, X-ray quality crystals of **3** were recovered in nearly quantitative yield from the reactions with TEMPO. Such reactivity appears counter-intuitive, as the slightly bulkier isopropyl R group could stabilize any organic radical intermediate. The inertness of **3** towards TEMPO suggests that the electronics of the Fe centers in the cluster is not the primary driving force of C–H atom abstraction. Rather, the driving force of the reaction is likely the peculiar susceptibility of the methyl C–H σ* orbital to TEMPO abstraction, as well as (in this case) the irreversible formation of gaseous byproducts.

In conclusion, we have demonstrated facile C–H atom abstraction from a methylthiolate-capped iron-carbonyl cluster (**1**); the isopropyl variant (**3**) is unreactive with TEMPO. H-atom abstraction from CH_3S^- ultimately results in the formation of an inorganic sulfide, which is incorporated to the product (**2**). Each starting cluster undergoes a one-electron oxidation and radical-assisted coupling of clusters, resulting in the S_2Fe_5 framework of the product dianion (**2**). This loosely resembles the SAM-mediated fusion of $[Fe_4S_4]$ clusters that ultimately comprise the nitrogenase active site. CO oxidation has been robustly characterized by identification of each TEMPO and cluster intermediate *en route* to CO_2. This result is of particular importance for future radical reactions attempting to generate a carbide, where utilization an iron-sulfur cluster not supported by carbonyls could minimize undesired side reactions. The fate of the methyl-carbon in this system is incorporation into multiple isotopic products, rather than carbon/carbide incorporation into the iron-sulfur-carbonyl cluster. We anticipate further mechanistic details in this system and *non-carbonyl* iron-sulfur clusters will be needed to shed further insight into the carbide insertion process during the formation of FeMoco.

Conflicts of interest

There are no conflicts to declare.

Acknowledgement

The authors acknowledge funding from the National Science Foundation (CHE-1808311) and the Welch Foundation (F-1822). We also thank Dr Vince Lynch for assistance in X-ray data collection and analysis.

Notes and references

(1) Spatzal, T.; Aksoyoglu, M.; Zhang, L.; Andrade, S. L. A.; Schleicher, E.; Weber, S.; Rees, D. C.; Einsle, O. Evidence for Interstitial Carbon in Nitrogenase FeMo Cofactor. *Science.* **2011**, *334* (6058), 940–942.

(2) Lancaster, K. M.; Roemelt, M.; Ettenhuber, P.; Hu, Y.; Ribbe, M. W.; Neese, F.; Bergmann, U.; DeBeer, S. X-Ray Emission Spectroscopy Evidences a Central Carbon in the Nitrogenase Iron-Molybdenum Cofactor. *Science.* **2011**, *334* (6058), 974–977.

(3) Rees, J. A.; Bjornsson, R.; Schlesier, J.; Sippel, D.; Einsle, O.;

DeBeer, S. The Fe-V Cofactor of Vanadium Nitrogenase Contains an Interstitial Carbon Atom. *Angew. Chem. Int. Ed.* **2015**, *54* (45), 13249–13252.

(4) Čorić, I.; Holland, P. L. Insight into the Iron-Molybdenum Cofactor of Nitrogenase from Synthetic Iron Complexes with Sulfur, Carbon, and Hydride Ligands. *J. Am. Chem. Soc.* **2016**, *138* (23), 7200–7211.

(5) Kuppuswamy, S.; Wofford, J. D.; Joseph, C.; Xie, Z. L.; Ali, A. K.; Lynch, V. M.; Lindahl, P. A.; Rose, M. J. Structures, Interconversions, and Spectroscopy of Iron Carbonyl Clusters with an Interstitial Carbide: Localized Metal Center Reduction by Overall Cluster Oxidation. *Inorg. Chem.* **2017**, *56* (10), 5998–6012.

(6) Joseph, C.; Kuppuswamy, S.; Lynch, V. M.; Rose, M. J. Fe_5Mo Cluster with Iron-Carbide and Molybdenum-Carbide Bonding Motifs: Structure and Selective Alkyne Reductions. *Inorg. Chem.* **2018**, *57* (1), 20–23.

(7) Liu, L.; Rauchfuss, T. B.; Woods, T. J. Iron Carbide–Sulfide Carbonyl Clusters. *Inorg. Chem.* **2019**, *58* (13), 8271–8274.

(8) Sickerman, N. S.; Ribbe, M. W.; Hu, Y. Nitrogenase Cofactor Assembly: An Elemental Inventory. *Acc. Chem. Res.* **2017**, *50* (11), 2834–2841.

(9) Wiig, J. A.; Hu, Y.; Ribbe, M. W. NifEN-B Complex of Azotobacter Vinelandii Is Fully Functional in Nitrogenase FeMo Cofactor Assembly. *Proc. Natl. Acad. Sci.* **2011**, *108* (21), 8623–8627.

(10) Wiig, J. A.; Hu, Y.; Lee, C. C.; Ribbe, M. W. Radical SAM-Dependent Carbon Insertion into the Nitrogenase M-Cluster. *Science.* **2012**, *337* (6102), 1672–1675.

(11) Wiig, J. A.; Hu, Y.; Ribbe, M. W. Refining the Pathway of Carbide Insertion into the Nitrogenase M-Cluster. *Nat. Commun.* **2015**, *6*, 1–6.

(12) Hu, Y.; Ribbe, M. W. Nitrogenases—A Tale of Carbon Atom(S). *Angew. Chem. Int. Ed.* **2016**, *55* (29), 8216–8226.

(13) Shupp, J. P.; Rose, A. R.; Rose, M. J. Synthesis and Interconversions of Reduced, Alkali-Metal Supported Iron-Sulfur-Carbonyl Complexes. *Dalton Trans.* **2017**, *46* (28), 9163–9171.

(14) Cherng, J.-J.; Tsai, Y.-C.; Ueng, C.-H.; Lee, G.-H.; Peng, S.-M.; Shieh, M. New Synthesis of $[SFe_3(CO)_9]^{2-}$ and Its Reactivity toward Electrophiles . *Organometallics* **2002**, *17* (2), 255–261.

(15) Kagalwala, H. N.; Lalaoui, N.; Li, Q. L.; Liu, L.; Woods, T.; Rauchfuss, T. B. Redox and "Antioxidant" Properties of $Fe_2(\mu\text{-}SH)_2(CO)_4(PPh_3)_2$. *Inorg. Chem.* **2019**, *58* (4), 2761–2769.

(16) Holliday, R. L.; Roof, L. C.; Hargus, B.; Smith, D. M.; Wood, P. T.; Pennington, W. T.; Kolis, J. W. The Chemistry of Iron Carbonyl Sulfide and Selenide Anions. *Inorg. Chem.* **1995**, *34* (17), 4392–4401.

(17) Calderoni, F.; Demartin, F.; Iapalucci, M. C.; Laschi, F.; Longoni, G.; Zanello, P. Synthesis and Chemical and Electrochemical Characterization of Fe-S Carbonyl Clusters. X-Ray Crystal Structures of $[N(PPh_3)_2]_2[Fe_5S_2(CO)_{14}]$ and $[N(PPh_3)_2]_2[Fe_6S_6(CO)_{12}]$. *Inorg Chem* **1996**, *35* (4), 898–905.

(18) Raal, F. A.; Danby, C. J.; Hinshelwood, C. The Reaction of Methyl Radicals with Olefins. Part III. *J. Chem. Soc.* **1949**, 2225–2230.

(19) Clark, T. C.; Izod, T. P. J.; Kistiakowsky, G. B. Reactions of Methyl Radicals Produced by the Pyrolysis of Azomethane or Ethane in Reflected Shock Waves. *J. Chem. Phys.* **1971**, *54* (3), 1295–1303.

(20) Ribeiro, J. M.; Mebel, A. M. Reaction Mechanism and Product Branching Ratios of the CH + C_3H_6 Reaction: A Theoretical Study. *J. Phys. Chem. A* **2016**, *120*, 1800–1812.

(21) Pacey, P. D.; Wimalasena, J. H. Kinetics and Thermochemistry of the Ethyl Radical. The Induction Period in the Pyrolysis of Ethane. *J. Phys. Chem.* **1984**, *88*, 5657–5660.

(22) Peukert, S. L.; Labbe, N. J.; Sivaramakrishnan, R.; Michael, J. V. Direct Measurements of Rate Constants for the Reactions of CH_3 Radicals with C_2H_6, C_2H_4, and C_2H_2 at High Temperatures. *J. Phys. Chem. A* **2013**, *117* (40), 10228–10238.

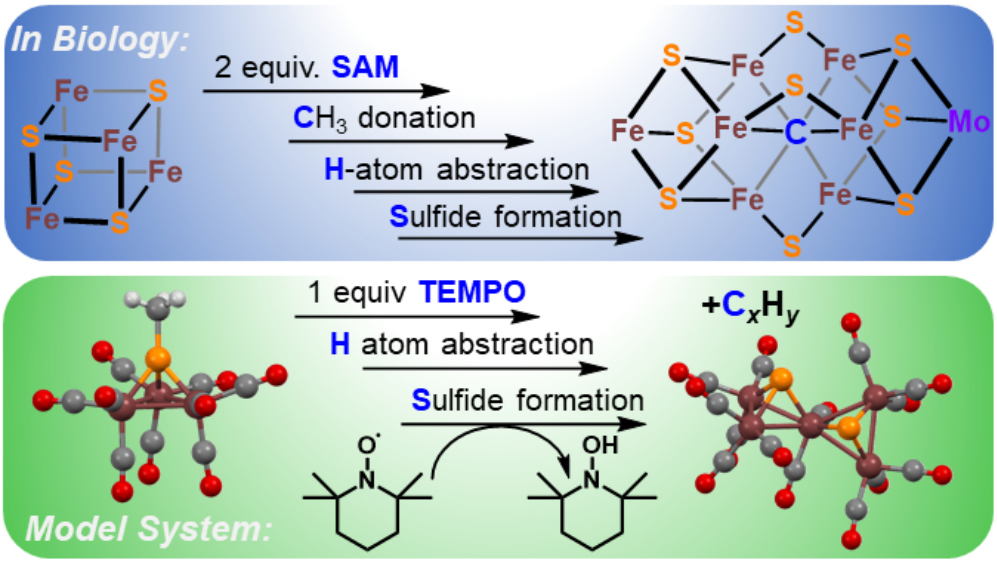

178x100mm (96 x 96 DPI)